Available online at www.sciencedirect.com

ScienceDirect

Procedia Materials Science 9 (2015) 335 – 340

Procedia Materials Science

www.elsevier.com/locate/procedia

International Congress of Science and Technology of Metallurgy and Materials, SAM – CONAMET 2014

Electrochemical tests in stainless steel surgical implants

Alex Kociubczyk[a,]*, Claudia Mendez[a], Ricardo Gregorutti[b], Alicia Ares[a]

[a]*Inst. de Mat. de Misiones (IMAM, CONICET-UNaM), FCEQyN, F. de Azara 1552, Posadas N3300LQH, Argentina*
[b]*Lab. de Entrenamiento Multidisciplinario para la Inv. Tecn. (LEMIT-CICPBA), Calle 52 esquina 121 y 122, La Plata B1900AYB, Argentina*

Abstract

In the present work the corrosion resistance of stainless steels was evaluated following the specifications of ASTM F-745 standards. The specimens were obtained by two methods, the conventional process of investment casting and countergravity low pressure casting. Cyclic polarization tests were performed according to ASTM F 2129, using a conventional three-electrode cell, with Pt as a counter electrode and saturated calomel as a reference electrode. The experiments were performed at (37 ± 1) ºC and, before starting the test, the electrolyte was purged with N_2 gas for 15 minutes. As electrolyte, a solution of 0.9% NaCl was used (pH≈7), the open circuit potential (OCP) was monitored for 1 hour and then the potentiodynamic scanning started in the anodic direction, at a speed of 0.167 mV/s, from a potential of 100 mV below the OCP. The sweep was reversed after passing the threshold of current density at a value hundred times greater than the current density of pitting. Measurements of electrochemical impedance spectroscopy were performed after one hour of exposure of the specimens to OCPs performed in a frequency range from 100 kHz to 1 mHz and potential amplitude of ± 10 mV. The microstructure of the samples was analyzed before and after testing using optical microscopy. The results indicated that the samples in general exhibit crack corrosion, and in some cases the occurrence of pitting corrosion was observed. Also, the capacity values were within the range corresponding to the electric double layer and the charge transfer resistance increased on the specimens obtained by conventional casting in ceramic mold.

Peer-review under responsibility of the Scientific Committee of SAM–CONAMET 2014

Keywords: Biomaterials; corrosion; stainless steel

* Corresponding author. Tel.: +54-376-442-2186; fax: +54-376-442-5414.
E-mail address: akociubczyk@fceqyn.unam.edu.ar

Peer-review under responsibility of the Scientific Committee of SAM–CONAMET 2014
doi:10.1016/j.mspro.2015.05.002

1. Introduction

Bioimplants are taking increasingly more importance to improve the lives of human beings, and it is commonly used in dentistry, orthopedics, reconstructive surgery, cardiovascular surgery, etc.

The alloys used for the construction of surgical implants must achieve certain requirements; the most important of them is the acceptability by the human body. The implanted material should not cause adverse effects such as allergy, inflammation and toxicity. Furthermore, the material should possess sufficient mechanical strength to withstand the forces to which they are subjected without breaking. One of the most important characteristics that a bioimplant should possess is a very high resistance to corrosion and wear in a highly aggressive physiological medium, such as the human body, which consists of blood and other components such as sodium, protein, minerals, anions (chlorides, phosphates, etc.), cations (Na^+, K^+, Ca^{2+}, etc.), dissolved oxygen, among others, Manivasagam et al. (2010) and Hansen et al. (2008).

In this work the austenitic stainless steel alloy was melted and solubilized according to ASTM F-745 specifications, which is one of the materials used for the manufacture of surgical implants by precision casting techniques, due to its excellent mechanical properties, high corrosion resistance, low cost and production capacity of large scale, ASTM international (2007) and Gregorutti et al. (2012).

The main variables that define the grain size, microstructure and macrosegregation are the temperature of the melt and the casting mold. Furthermore, the presence of oxygen in the atmosphere during the different steps of melting and casting of the parts induces the formation of nonmetallic inclusions. The presence of inclusions may induce mechanical fatigue failures, corrosion or a combination of both, Teoh (2000) and Sudhakar (2005).

The austenitic stainless steel alloys are susceptible to pitting corrosion and cracks. These localized corrosion attacks are the cause of most failures implants, these being the areas of active mechanisms where fatigue cracks are initiated by Altobelli Antunes et al. (2012).

The aim of this paper is to evaluate and compare the corrosion resistance through cyclic polarization (CP), electrochemical impedance spectroscopy (EIS) and open circuit potential (OCP) techniques in stainless steels obtained according to the specifications of ASTM F-745. The specimens were obtained by investment casting (IC) and countergravity low pressure casting (CLA) solidification techniques.

2. Experimental

2.1. Casting methods

The chemical composition of stainless steel used in this work is: Fe-21Cr-0.042C-9.34Ni-2.13Mo-1.26Mn-0.69Si-0.5N (% by weight). The casting was performed using an induction furnace of 30 kg capacity.

As usual practice of the IC process, the ceramic mold was preheated to 800 °C to increase its permeability and reduce the thermal gradient during the cooling, in order to improve castability. Filling is performed by gravity through a spoon. Moreover, CLA process was conducted by placing the preheated shell (100 °C to remove moisture) in a casting chamber connected to a vacuum pump. In this process, the shell mold was filled by suction directly from the induction furnace, due to the pressure difference caused by the vacuum.

2.2. Heat treatment

Solubilized heat treatment was performed to dissolve the δ-ferrite and carbides. The thermal cycle consisted of heating to 1080 °C for one hour under normal atmospheric conditions, and subsequent water quench.

2.3. Sample preparation

The surface of specimens (corresponding to the sides exposed to body fluids) was isolated with epoxy resin, then it was grinded with SiC abrasive paper of different grain sizes (#120-#2500), under constant water flow, and was rapidly cleaned with water and alcohol and dried with hot air.

2.4. Cyclic potentiodynamic tests

Cyclic potentiodynamic tests were performed according to ASTM F-2129, using a conventional three-electrode cell, using Pt electrode as a counter electrode and a saturated calomel (SCE) as a reference electrode. Measurements were made with a potentiostat / galvanostat / ZRA GAMRY® reference 600. The experiments were performed at 37 °C, before starting the test solution was purged with N_2 gas for 15 minutes. Electrolyte solution 0.9% NaCl (pH≈7) was used. Open circuit potential (OCP) was monitored for 1 hour and then the potentiodynamic scanning started in the anodic direction, at a speed of 0.167 mV/s from a potential of 100 mV below the OCP. The sweep was reversed after passing the threshold current density at a value of two greater than the current density of pitting decades.

2.5. Electrochemical impedance spectroscopy (EIS)

Measures of electrochemical impedance spectroscopy were performed after one hour exposure of the samples to OCP, using a frequency range of 100 kHz to 1 mHz and potential amplitude of ± 10 mV.

3. Results and discussion

3.1. Cyclic potentiodynamic curves

In Fig. 1, the cyclic potentiodynamic curves for the different parts of the prothesis (femoral stem (FS) and femoral head (FH)) are compared.

The main characteristics to evaluate this technique are the potential breakdown of the passive film (E_{pit}) and the potential at which it becomes to form the the passive film (E_b). E_{pit} is the potential level at which the current increases significantly. In turn, E_b is the potential at which the hysteresis loop is completed in the reverse polarization scan. A material having more electropositive potential, i.e. when the difference (E_{pit}-E_{corr}) is greater and the difference between (E_{pit}-E_b) is lower, will be less susceptible to localized corrosion.

We can observe that for the specimens obtained by CLA, the corrosion potential is greater in the header area of the femoral stem while the pitting potential is more electropositive on the stem. However, we can see

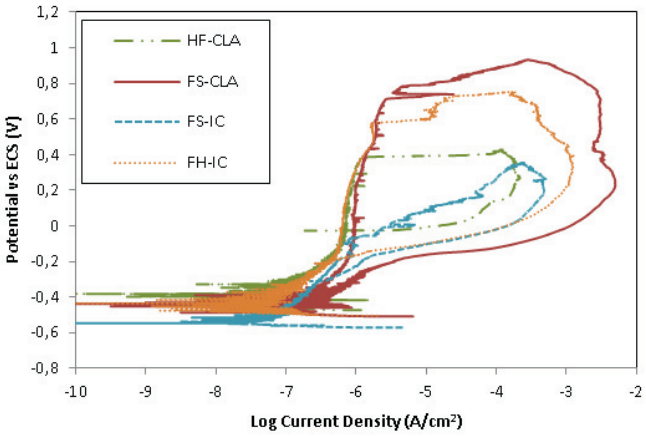

Fig. 1. Cyclic potentiodynamic curves of alloy corresponding to ASTM F745.

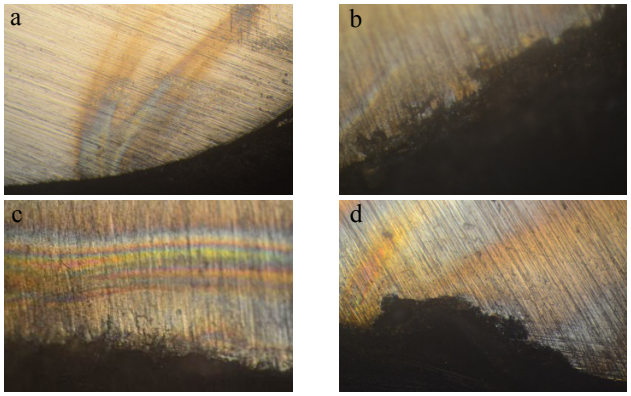

Fig. 2. Optical microscopy pictures (magnification:10X), (a) FH-CLA; (b) FS-CLA; (c) FH-CI; (d) FS-IC.

that the femoral head shows a repassivation at a potential of -0.07 V, whereas the stem has not achieved a repassivation. On the other hand, we can see that the difference (E_{pit}-E_{corr}) in the femoral stem is almost the double of that obtained in the femoral head, thus offering a wide range of potentials for which the metal is passive.

In the specimens obtained by conventional casting in the ceramic mold we can see that the corrosion potential behaves similarly to CLA, being greater in the header area of the femoral stem. However, the behavior of the pitting potential is different, being more electropositive in the head area. Also, we can see that the difference (E_{pit}-E_{corr}) in the femoral head twice of that obtained in the femoral stem, thus offering a wide range of potentials for which the metal is passive, as said before. Furthermore, the spindle has a higher repassivation potential than the stem.

We can also consider the level of passive currents, in this case begin is slightly lower for the IC method than for CLA.

Fig. 2 shows the appearance of crevice corrosion in all experiences. Electrochemical parameters obtained from potentiodynamic curves are presented in Table 1.

Table 1. Electrochemical parameters obtained from potentiodynamic curves.

Material	Parameter				
	E_{corr} (V vs SCE)	E_{pit} (V vs SCE)	(E_{pit}-E_{corr}) (V)	E_b (V vs SCE)	(E_{pit}-E_b) (V)
FS-IC	-0.539	-0.107	0.432	-0.305	0.198
FH-IC	-0.452	0.527	0.979	-0.182	0.709
FS-CLA	-0.438	0.741	1.179	-	-
FH-CLA	-0.382	0.358	0.740	-0.077	0.435

3.2. Electrochemical impedance spectroscopy (EIS)

Impedance diagrams were obtained for two different castings in the test areas. The analyzed surface was that which was in contact with body fluids. Nyquist and Bode plots are shown in Figs. 3 and 4. Fig. 3 shows the presence of a simple capacitive arc obtained from a specimen of CLA femoral head area. This behavior is similar in each of the tested areas corresponding to different castings and corresponds to a simple electronic model. This model is represented by a connected resistor, Rs, in series with a parallel combination of a resistance, Rp, and a constant phase element (CPE), with values of n approaching unity, so that it behaves as a capacitance, as shown in Fig. 5.

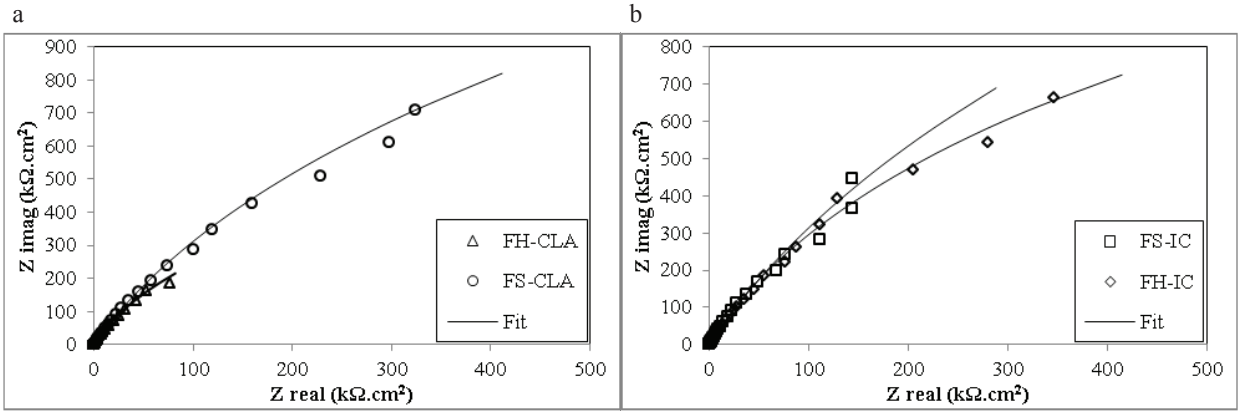

Fig. 3. Nyquist plots. (a) CLA; (b) IC.

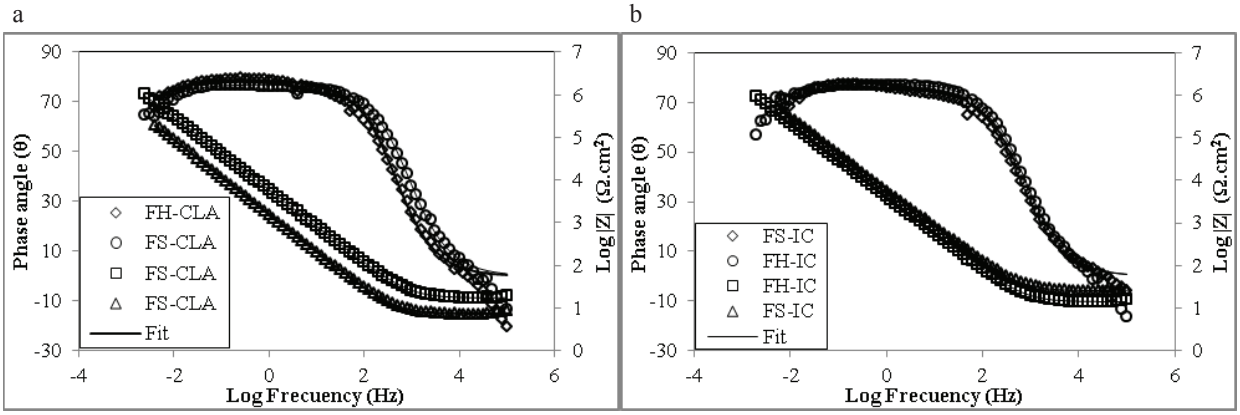

Fig. 4. Bode plots. (a) CLA; (b) IC.

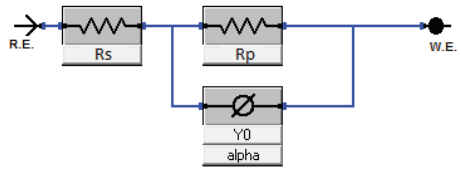

Fig. 5. Equivalent electronic circuit.

The solution resistance, Rs, was obtained by performing a scan at high frequencies. Furthermore, Rp is the resistance term of load transfer and corresponds to the diameter of the semicircle from the Nyquist plots in Fig. 3. The interactions produced at the electrode / electrolyte are related to the double layer capacitance, Cp, Sobral et al. (2001).

Both the impedance module and the phase angle show a shift towards lower frequencies, a phenomenon that has an associated increase in capacitance, which is related to an increased of effective surface area. This phenomenon is observed when comparing the results between the two FH and FS zones in each of the castings. Furthermore, the

identity coefficient, n, decreases in the region of the shaft, which indicates that it has a less smooth surface. The electrochemical parameters obtained from EIS curves are presented in Table 2.

Table 2. Electrochemical parameters obtained from EIS.

Material	Parameter			
	Rp ($\Omega.cm^2$)	Rs ($\Omega.cm^2$)	Cp ($\mu F/cm^2$)	n
FS-IC	3039317.64	36.50	71.39	0.848
FH-IC	3174518.11	16.56	25.16	0.865
FS-CLA	5651318.38	26.19	26.08	0.857
FH-CLA	2434875.07	13.16	46.24	0.874

4. Conclusion

The results show that the ASTM F-745 stainless steel is susceptible to crevice corrosion and pitting. CLA generally has a lower susceptibility to localized corrosion.

In CLA the femoral stem is the area with greater corrosion resistance; this is because the metallurgical quality of the cast steel is much better in vacuum conditions, presenting fewer inclusions and smaller grain size. IC in the femoral head has better corrosion resistance.

In both castings, the femoral head zone is the one showing a larger heterogeneous surface with greater effective surface.

Acknowledgements

The authors thank the Consejo Nacional de Investigaciones Científicas y Técnicas (CONICET), Buenos Aires, Argentina, the National University of Misiones, Misiones, Argentina, and the staff of Laboratorio de Entrenamiento Multidisciplinario para la Investigación Tecnológica (LEMIT-CICPBA), La Plata, Argentina. Also, the authors aknowledge to FONCyT-ANPCyT, Argentina, for funds received through PICT-2014-0170.

References

R. Altobelli Antunes, M. C. Lopes de Oliveira, 2012. Corrosion-fatigue of biomedical metallic alloys: Mechanisms and mitigation. Acta Biomaterials 8, 937–962.

ASTM F745-07, 2007. ASTM International, Section 13, 302–304.

R. W. Gregorutti, J. E. Grau, C. I. Elsner, 2012. Microstructural, mechanical and electrochemical characterisation of biomaterial ASTM F745 cast by vacuum. Materials Science and Technology, Vol. 28, Nº6, 742-747.

D. C. Hansen, 2008. Metal Corrosion in the Human Body: The Ultimate Bio-Corrosion Scenario. The Electrochemical Society Interface, Vol. 17, Nº2, 31-34.

G. Manivasagam, D. Dhinasekaran, A. Rajamanickam, 2010. Biomedical Implants: Corrosion and its Prevention - A Review. Recent Patents on Corrosion Science, Vol. 2, 40-54.

A.V.C. Sobral, W. Ristow, D.S. Azambuja, I. Costa, C.V. Franco, 2001. Potentiodynamic tests and electrochemical impedance spectroscopy of injection molded 316L Steel in NaCl solution. Corrosion Science 43, 1019-1030.

K. V. Sudhakar, 2005. Metallurgical investigation of a failure in 316L stainless steel orthopaedic implant. Engineering Failure Analysis 12, 249–256.

S. H. Teoh, 2000. Fatigue of biomaterials: A review. International Journal of Fatigue 22, 825–837.